ACS APPLIED MATERIALS & INTERFACES

Research Article

www.acsami.org

Nanostructured Titanium Nitride/PEDOT:PSS Composite Films As Counter Electrodes of Dye-Sensitized Solar Cells

Hongxia Xu,[†,‡] Xiaoying Zhang,[†,§,‡] Chuanjian Zhang,[†,§] Zhihong Liu,[†] Xinhong Zhou,[⊥] Shuping Pang,[†] Xiao Chen,[†] Shanmu Dong,[†,§] Zhongyi Zhang,[†,§] Lixue Zhang,[†] Pengxian Han,[†] Xiaogang Wang,[†] and Guanglei Cui*[,†]

[†]Qingdao Institute of Bioenergy and Bioprocess Technology, Chinese Academy of Sciences, Qingdao 266101, P. R. China

[§]Graduate School of the Chinese Academy of Sciences, Beijing, 100080, P. R. China

[⊥]Qingdao University of Science and Technology, Qingdao, 266101, P. R. China

Supporting Information

ABSTRACT: The composite films of titanium nitride in conjunction with polystyrenesulfonate-doped poly (3,4-ethylene-dioxythiophene) (PEDOT:PSS) were prepared by a simple mechanical mixture of TiN and PEDOT:PSS under ultrasonication, which was demonstrated to deliver an effectively combined network of both high electrical conductivity and superior electrocatalytic activity. The composite films have been explored as an alternative for the counter electrodes of dye-sensitized solar cells. It was manifested that these nanostructured TiN-PEDOT:PSS composite films displayed excellent performance comparable to Pt-FTO counter electrode due to the combined network endowing more favorable and efficient interfacial active sites. Among them, the energy conversion efficiency of the cell with TiN(P)-PEDOT:PSS as counter electrode reached 7.06%, which was superior to 6.57% of the cell with Pt-FTO counter electrode under the same experimental conditions.

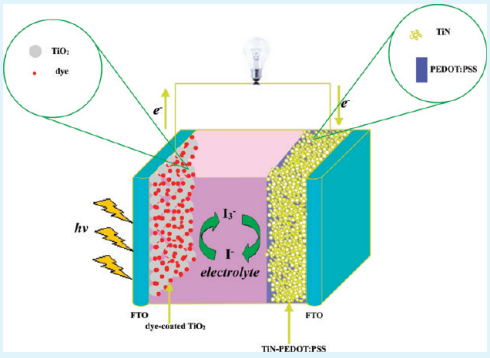

KEYWORDS: *nanostructured titanium nitride, polystyrenesulfonate-doped poly (3,4-ethylene-dioxythiophene), composite film, counter electrode, dye-sensitized solar cell, photovoltaic performance*

INTRODUCTION

Dye-sensitized solar cells (DSSCs) introduced by Grätzel and O'Regan two decades ago have been investigated extensively because of DSSCs presenting some advantages over traditional Si-solar cells such as low production cost and relatively high light-to-electricity conversion efficiency (η) and easy scale-up.[1−5] However, further enhancement in conversion efficiency and decrease in production cost are highly desired for large-scale fabrication of DSSCs.

As an important component in DSSCs, the counter electrode (CE) collects electrons from the external circuit, transfers them back to the redox electrolyte, and catalyzes the reduction of triiodide ions to iodide ions, which makes the cell a complete circuit. Therefore, the counter electrode materials should possess high electrical conductivity and superior electrocatalytic activity to decrease the overvoltage to minimize the energy losses.[6] Typically, the counter electrodes in DSSCs are usually made of the noble metal platinum (Pt). However, Pt may limit the potential large scale applications because of the natural scarce and possible dissolution in LiI/I_2 solution.[7] It is highly imperative to explore low-cost, abundant, and highly efficient substitutes for the conventional Pt counter electrode in the DSSC system. To reduce the cost of the CE, several kinds of fascinating substitutes such as carbonaceous materials[8−12] and conductive polymer[13,14] have been investigated as CEs to replace platinum in DSSCs. Unfortunately, these materials suffered from low intrinsic electrocatalytic activity in reducing triiodide.

Recently, metallic compounds (metal nitrides,[15−17] metal carbides,[18,19] metal sulfides[20]) with similar properties to those of noble metals have been proposed to replace the conventional Pt CE. Some of metallic compounds based materials such as TiN showed an excellent performance comparable to typical Pt counter electrode. However, metallic compound nanoparticles such as TiN nanoparticles suffered from aggregation resulting in lower catalytic surface, poor conductivity and weak bonding to the FTO substrate and finally yielding lower fill factor (*FF*) because of the poor electron transport efficiency between nanoparticles and substrate.[17] To address these issues mentioned above, electronic nanowiring by conductive polymer[21] or carbon coating[22] may be a better alternative, which also endows an effective combined network of both high electrical conductivity and superior electro-catalytic activity. It was reported that polystyrenesulfonate-doped poly (3, 4-

Received: December 6, 2011
Accepted: January 20, 2012
Published: January 20, 2012

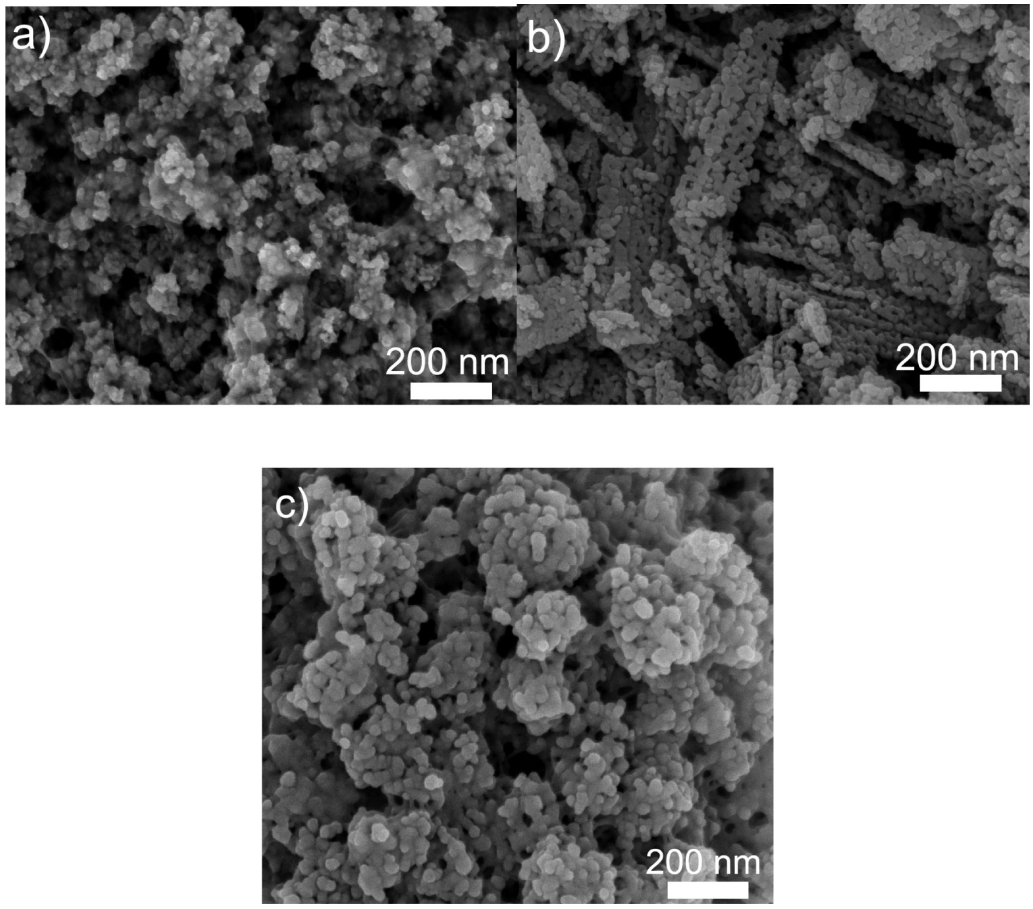

Figure 1. Typical SEM images of the TiN-PEDOT:PSS composite films. (a) TiN(P)-PEDOT:PSS, (b) TiN(R)-PEDOT:PSS, and (c) TiN(S)-PEDOT:PSS.

ethylenedioxythiophene)(PEDOT:PSS) possesses high conductivity (up to 550 S/cm when highly doped), excellent electrocatalytic activity for the reduction of triiodide ions to a certain extent, good binding ability.[23] The strategy of incorporating inorganic nanostructured materials into PEDOT:PSS has been proved to fabricate highly efficient and low-cost counter electrode materials for DSSCs.[24] Therefore, the composite films of titanium nitride and PEDOT:PSS are expected to exhibit improved performance as promising candidate counter electrodes of DSSCs because of a fast electron transport network with highly active sites on the electron transport pathway.

Herein, we presented a simple mechanically mixing process followed by ultrasonic treatment for preparation of hybrids of TiN and PEDOT-PSS (TiN-PEDOT:PSS). It was expected that the DSSCs with the composite films as counter electrodes exhibited superior photovoltaic performance comparable to those of Pt-FTO.

EXPERIMENTAL SECTION

Materials. Titanium nitride nanoparticles (TiN(P)) was purchased from Hefei kaier nanometer energy and technology Co., Ltd., China and ground with a mortar and pestle. A commercial aqueous dispersion of PEDOT:PSS (polymer concentration of 2.2−2.6%, high conductive grade) was purchased from Sigma-Aldrich and used as received without further purification. Iodine and 4-tert-butylpyridine were purchased form TCI. N719 dye $(Ru(dcbpy)_2(NCS)_2$(dcbpy =2,2-bipyridyl-4,4-dicarboxylato) was purchased from Solaronix. TiO_2 paste was purchased from Dalian HeptaChroma SolarTech Co., Ltd., China.

Synthesis of TiN Nanorods (TiN(R)) and TiN Mesoporous Spheres (TiN(S)). In a typical synthesis, commercial Degussa P25 powder (0.5 g) was mixed with aqueous NaOH (10 M) and absolute ethanol with a volume ratio of 1:1. Then the mixed solution (20 mL) was transferred into a 100 mL Teflon-lined stainless steel autoclave. The autoclave was maintained at 170−200 °C under autogenous pressure for 24 h and then cooled to room temperature naturally. The obtained sample was filtered off, washed several times with dilute HCl aqueous solution and deionized water until the pH value of the solution was about 7. The as-prepared TiO_2 was dried at 60 °C for 12 h in air and then heated to 800 °C under ammonia for 1 h with a progressive, slow heating ramp (room temperature to 300 °C, 5 °C min^{-1}; 300 to 700 °C, 2 °C min^{-1}; 700 to 800 °C, 1 °C min^{-1}). After being cooled to room temperature, TiN(R) were finally obtained as the resultant black powders. TiN(S) were fabricated according to our previous work.[25]

Preparation of Counter Electrodes. The mirrorlike Pt/FTO electrode was obtained by electrodepositing a platinum layer on the surface of fluorine-doped tin oxide substrate. The thickness of Pt films is about 75 nm. The milled TiN (50 mg) were dispersed with the PEDOT:PSS aqueous solution (200 mg), then ultrasonically dispersed for 30 min, resulting in the homogeneous paste (TiN-PEDOT:PSS) containing TiN and PEDOT:PSS. Although TiN paste was prepared by ultrasonically dispersing in the water for 30 min. The counter electrode films were prepared on precleaned fluorine-doped tin oxide (FTO) substrate by doctor blade technique followed by heat drying at 110 °C for 10 min.

Fabrication of DSSCs. TiO_2 working photoanodes were prepared on FTO substrate using TiO_2 paste by doctor blade technique and subsequently sintered at 500 °C for 30 min in air. The resultant TiO_2

photoanodes were soaked in an ethanol solution of N719 dye (3×10^{-4} M) for 24 h to obtain dye-sensitized TiO_2 electrode. The dye-adsorbed TiO_2 photoanodes with an active area of 0.2 cm^2 were assembled with TiN, TiN-PEDOT:PSS, and platinum counter electrodes using laboratory tape as a spacer to fabricate corresponding sandwich-type cells, respectively. The liquid electrolyte is composed of 0.3 M 1,2-dimethyl-3-propylimidazolium iodide (DMPII), 0.05 M iodine (I_2), 0.5 M lithium iodide (LiI), and 0.5 M 4-*tert*-butylpyridine (TBP) with acetonitrile (ACN) as the solvent.

Characterization. The morphologies of the TiN(R), TiN(S), TiN-PEDOT:PSS composite films were investigated using field-emission scanning electron microscopy (FESEM HITACHI S-4800). X-ray diffraction (XRD) patterns were recorded with a Bruker-AXS Microdiffractometer (D8 ADVANCE) using Cu Ka radiation (λ = 1.5406 Å) from 5 to 95 °C. Cyclic voltammetry (CV) was carried out in a three-electrode system in an acetonitrile solution of 0.1 M $LiClO_4$, 10 mM LiI, and 1 mM I_2. Platinum served as a counter electrode and the nonaqueous Ag/Ag^+ couple was used as a reference electrode. The photocurrent–voltage characteristics of the DSSCs were measured with a Newport (USA) solar simulator (300 W Xe source) and a Keithley 2420 source meter. Electrochemical impedance spectroscopy (EIS) measurements were performed using a Zahner Ennium electrochemical workstation by applying an AC voltage of 10 mV amplitude in the frequency range between 100 kHz and 100 mHz at room temperature. Fitting of impedance spectra to the proposed equivalent circuit was performed by using the Zsimpwin software.

RESULTS AND DISCUSSION

Morphology. Surface morphologies of TiN(P)-PEDOT:PSS composite films, TiN(R)-PEDOT:PSS composite films and TiN(S)-PEDOT:PSS composite films on fluorine-doped tin oxide (FTO) glass substrates were depicted in Figure 1. It was showed that TiN(P) were dispersed uniformly in the PEDOT:PSS matrix, which was beneficial to electronic conduction. For TiN(R), PEDOT:PSS interconnected one-dimensional TiN rod with nanoparticles size of approximately 20 nm and covered in the surface of 20–50 nm porous structures (see Figure S1a in the Supporting Infomration). TiN mesoporous spheres with the spherical diameters of about 170 ± 20 nm were linked by PEDOT:PSS where the size of TiN mesoporous spheres primary nanoparticles is in the range between 10 and 20 nm (see Figure S1b in the Supporting Information). It can be seen in Figure 1, the uniformity of TiN(P)-PEDOT:PSS is much higher than that of TiN(R)-PEDOT:PSS and TiN(S)-PEDOT:PSS which presented much more catalytic sites. The resultant composite films were mechanically enough stable not to peel from the FTO substrate compared with pristine TiN films. The thickness of these counter electrodes was controlled to be 6 μm.

Electrochemical Analysis. Cyclic voltammetry (CV) was carried out to evaluate the electrocatalytic activity of several kinds of counter electrodes to reduce triiodide under the same conditions. Figure 2 exhibits cyclic voltammograms for I_3^-/I^- redox reaction obtained on TiN(P)-PEDOT:PSS, TiN(R)-PEDOT:PSS, TiN(S)-PEDOT:PSS and Pt electrodes at a scan rate of 20 mV s^{-1}. The Pt electrodes display two typical pairs of peaks,[26] where the relative negative pair is assigned to the redox equation eq 1 and the positive pair is ascribed to redox reaction eq 2.[27] These composite films of TiN(P)-PEDOT:PSS, TiN(R)-PEDOT:PSS, TiN(S)-PEDOT:PSS present two pairs of well-defined peaks and similar peak potential to Pt, which indicate an excellent electrocatalytic characteristic as Pt. The value of peak separation (ΔE_p) is 0.449 v for TiN(S)-PEDOT:PSS, 0.249 v for TiN(R)-PEDOT:PSS, 0.265 v for TiN(P)-PEDOT:PSS, 0.257 v for Pt, respectively. It is deduced

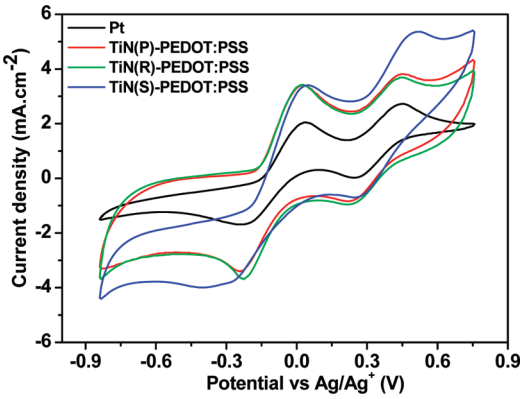

Figure 2. Cyclic voltammograms of Pt, TiN(P)-PEDOT:PSS, TiN(R)-PEDOT:PSS, TiN(S)-PEDOT:PSS counter electrodes in 10 mM LiI, 1 mM I_2 and 0.1 M $LiClO_4$ acetonitrile solution at a scan rate of 20 mV s^{-1}.

that the electron transfer rate of TiN(R)-PEDOT:PSS and TiN(P)-PEDOT:PSS is comparable to Pt. The larger ΔE_p for TiN(S)-PEDOT:PSS indicates that electron transfer rate of TiN(S)-PEDOT:PSS is lower than that of Pt according to previous literatures.[28] In addition, TiN-based composite electrodes exhibit a higher current density over Pt-FTO demonstrating more electrochemical catalytic sites owing to the synergetic structure of the composite. For a fair comparison, TiN(P), TiN(R), TiN(S), and PEDOT:PSS were also evaluated by CV (see Figure S3 in the Supporting Information). Although it was reported TiN possessed good electrocatalytic activity for reduction of I_3^-,[17] TiN(P) electrodes in our case display negligible oxidation/reduction peaks of I_3^-, which could be ascribed to the poor electron transport between TiN nanoparticles. TiN(R) and TiN(S) electrodes are demonstrated to show an improved performance than TiN(P) due to efficient electron transport and nonfaradaic current caused by the porous electrodes. The pristine PEDOT:PSS electrodes do not present well-defined peaks due to low reduction reaction rate, which is consistent with previous report.[29]The improved current density of TiN-based composite electrodes compared with TiN based electrodes is partly ascribed to more effective conductive network of PEDOT:PSS bridge between TiN. The CV results indicate that TiN-PEDOT:PSS composite films can be potential as efficient counter electrodes of DSSCs. The above discrepancy as measured by CV is supposed to directly influence the photovoltaic performance of DSSC, as shown hereinafter.

$$I_3^- + 2e^- \rightleftharpoons 3I^- \quad (1)$$

$$3I_2 + 2e^- \rightleftharpoons 2I_3^- \quad (2)$$

The photocurrent density–voltage (J–V) characteristic curves of the DSSCs fabricated with different composite counter electrodes measured under the illumination of 1 sun (100 mW cm^{-2}) are shown in Figure 3. The TiN(P)-PEDOT:PSS based devices yield energy conversion efficiencies of 7.06%, which is superior to that of Pt–FTO devices (6.57%). Meanwhile, the energy conversion efficiency is improved to 6.89% for TiN(R)-PEDOT:PSS, 6.19% for TiN(S)-PEDOT:PSS, respectively. For a fair comparison, the J–V curves of the DSSCs using TiN based counter electrodes are presented. The devices using pristine TiN nanoparticles in the absence of PEDOT:PSS exhibit a very low *FF* (11.36%)

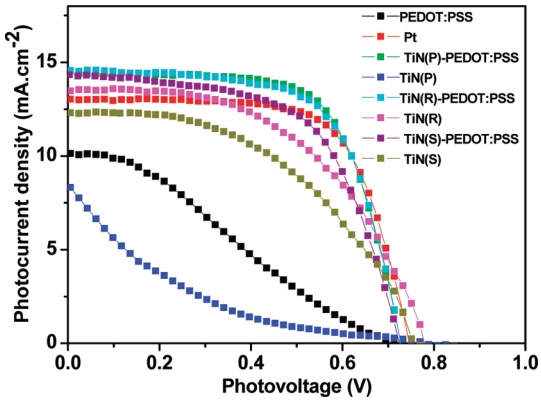

Figure 3. Characteristic photocurrent density–voltage (J–V) curves of DSSCs with different electrodes, measured under simulated sunlight 100 mW cm^{-2} (AM 1.5). The liquid electrolyte is composed of 0.05 M I_2, 0.1 M LiI, 0.6 M 1,2-dimethyl-3-propylimidazolium iodide (DMPII), and 0.5 M 4-*tert*-butyl pyridine in acetonitrile solution.

because of poor electron transport through TiN grain boundaries between TiN nanoparticles, which yield a poor photovoltaic performance (0.76%). It is also observed that the pristine PEDOT:PSS based devices achieve a conversion efficiency of 2.04% possibly due to low specific surface area. In comparison with TiN(P), TiN(R)- and TiN(S)-based devices deliver better photovoltaic performance (5.43% for TiN(R), 4.49 for TiN(S)) because of their excellent electronic and electrocatalytic network. It is noted that the TiN(R) based devices show higher photocurrent density than that with TiN(S), possibly because of the fast electron transfer rate of one-dimensional structure, which is in good accordance with the CV analysis. It is supposed that the overall characteristics of TiN-PEDOT:PSS composite counter electrode reveal predominant synergistic effect of TiN and PEDOT:PSS because of the more favorable electrical conductivity and electrocatalytic activity for the reduction of triiodide to iodide.

The photovoltaic parameters of these devices, including the short-circuit current (J_{sc}), the open-circuit voltage (V_{oc}), the fill factor (FF), and the energy conversion efficiency (η), are summarized in Table 1. It is indicated that the enhanced

Table 1. Characteristics of the J–V Curves of the DSSCs Fabricated Using Different Counter Electrodes

counter electrode	J_{sc} (mA/cm^2)	V_{oc} (mV)	*FF* (%)	η (%)
TiN(P)	8.51	789	11.36	0.76
TiN(P)-PEDOT:PSS	14.45	727	67.18	7.06
TiN(R)	13.49	782	51.46	5.43
TiN(R)-PEDOT:PSS	14.53	727	65.26	6.89
TiN(S)	12.24	764	47.95	4.49
TiN(S)-PEDOT:PSS	14.35	724	59.48	6.18
PEDOT:PSS	10.09	713	28.41	2.04
Pt	13.09	746	67.31	6.57

performance of TiN-PEDOT:PSS electrodes over TiN electrode arise from the higher J_{sc} and *FF*. The improvement of J_{sc} in composite electrodes can be mainly ascribed to a more efficient electrochemical catalytic activity due to electronic nanowiring of PEDOT:PSS between TiN. It is worthwhile to note that more than 50 mV drop in the open-circuit voltage is observed after compositing the PEDOT:PSS with TiN. As it was reported, higher electrocatalytic activity of counter electrode could improve distribution of electron state density in the TiO_2 electrode,[30] which could cause an increase in the recombination possibility resulting in decreased V_{oc} of the TiN composite based devices. This is verified with our dark current measurement (Figure 4). It is concluded that the enhanced

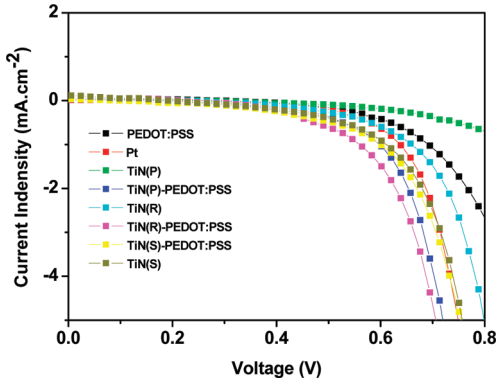

Figure 4. Characteristic current density–voltage (J–V) curves of DSSCs with different electrodes, measured under dark condition. The liquid electrolyte is composed of 0.05 M I_2, 0.1 M LiI, 0.6 M 1,2-dimethyl-3-propylimidazolium iodide (DMPII), and 0.5 M 4-*tert*-butyl pyridine in acetonitrile solution.

performance of composite is mainly due to that PEDOT:PSS nanowiring TiN, delivering a fast electro-transport network combined with highly active sites on the electron transport pathway.[24]

In order to further evaluate the electrochemical activity of the composite materials as counter electrodes in DSSCs, the electrochemical impedance spectra (EIS) were measured in a symmetric sandwich cell configuration consisting of two identical counter electrodes. Their Nyquist plots are illustrated in Figure 5. For TiN(P)-PEDOT:PSS, TiN(R)-PEDOT:PSS,

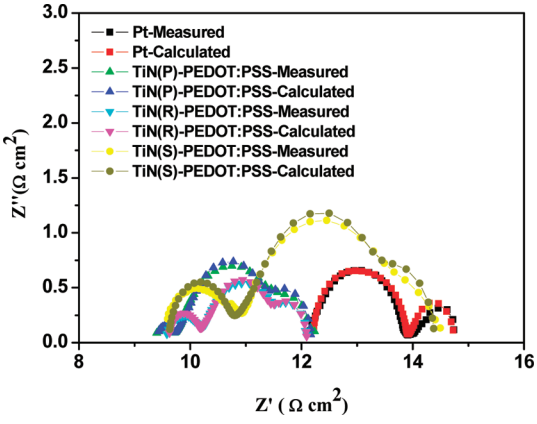

Figure 5. Nyquist plots and corresponding simulation results of the symmetric cells with two identical counter electrodes of Pt (black square, measured; red square, calculated), TiN(P)-PEDOT:PSS (green triangle, measured; dark blue triangle, calculated), TiN(R)-PEDOT:PSS (light blue triangle, measured; purple triangle, calculated), TiN(S)-PEDOT: PSS (yellow circle, measured; tan circle, calculated). The cells were measured with the frequency range between 100 kHz and 100 mHz.

and TiN(S)-PEDOT:PSS, three semicircles are visible due to porous structures of materials. The semicircle in the high-frequency region corresponds to the charge-transfer resistance

of counter electrode/redox (I^-/I_3^-) interface and the capacitance of the counter electrode/electrolyte interface,[31] and the one in the middle frequency region is associated with the adsorption of iodine and triiodide on the electrode surface with large active areas. The low-frequency semicircle is attributed to the Nernst diffusion impedance of the I^-/I_3^- redox species within a thin layer in the electrolyte, whereas the high frequency offset determines the series resistance.[16] The equivalent circuit used is given in Figure S5 in the Supporting Information and the simulated data from the EIS spectra for TiN-PEDOT:PSS and Pt are summarized in Table 2. The

Table 2. EIS Parameters of the Symmetric Cells Based on Different Counter Electrodes

counter electrode	R_s (Ω cm^2)	R_{ct} (Ω cm^2)	C (μF cm^{-2})
TiN(P)-PEDOT:PSS	9.39	0.28	13.03
TiN(R)-PEDOT:PSS	9.61	0.51	17.22
TiN(S)-PEDOT:PSS	9.62	1.06	13.05
Pt	12.2	1.14	13.38

others are presented in Table S1 in the Supporting Information. The simulated charge-transfer resistances of TiN(P)-PEDOT:PSS, TiN(R)-PEDOT:PSS and TiN(S)-PEDOT:PSS counter electrode are 0.28, 0.51, and 1.06 Ω cm^{-2}, respectively, much lower than that of Pt electrode (1.14Ω cm^{-2}), suggesting the superior electrocatalytic activity of the composite electrodes over Pt-FTO electrode for the reduction of triiodide ions. The electrocatalytic activity of TiN(P)-PEDOT:PSS (0.28 Ω cm^{-2}), TiN(R)-PEDOT:PSS (0.51 Ω cm^{-2}) and TiN(S)-PEDOT:PSS (1.06 Ω cm^{-2}) is better than pristine TiN material according to their charge-transfer resistance compared with 1.79 Ω cm^{-2} of TiN(P), 1.48 Ω cm^{-2} of TiN(R), and 1.38 Ω cm^{-2} of TiN(S), indicating the compositing of TiN and PEDOT:PSS could deliver a synergistic effect to improve electrocatalytic activity of I^-/I_3^- redox species. The R_s values of TiN composite film electrodes are also much lower than that value of the TiN electrode and Pt. This could be attributed to the robust bonding between the TiN composite film and the FTO substrate, which is proofed by a previous report.[15] The higher R_s values maybe result in smaller J_{sc} value of the DSSCs with the Pt counter electrode than that of the DSSCs with the TiN composite counter electrodes.[32] The lower resistance would endow a greater FF and higher η in solar cell, which is corroborated by the corresponding performance measurement.

CONCLUSION

In summary, dye-sensitized solar cells with nanostructured TiN and PEDOT:PSS composite films as the counter electrode were explored, which were fabricated by a simple mixture of nanostructured TiN and PEDOT:PSS under ultrasonication followed by a doctor-blade. The composite counter electrode was demonstrated to display superior photovoltaic performance comparable to a conventional Pt counter electrode due to the formation of highly efficient electron transfer network. The TiN nanostructure was also varied to explore highly efficient electron transfer network and optimize better photovoltaic performance of DSSCs. We believe that the current work paves the way for the compositing nanostructured material, which is promising for fabricating highly efficient and low-cost counter electrode for DSSCs.

ASSOCIATED CONTENT

Supporting Information

TEM and XRD of TiN(R) and TiN(S), cyclic voltammograms of PEDOT:PSS, TiN(P), TiN(R), TiN(S) counter electrodes, Nyquist plots of different counter electrodes and equivalent circuit for the EIS. This material is available free of charge via the Internet at http://pubs.acs.org/.

AUTHOR INFORMATION

Corresponding Author

*E-mail: cuigl@qibebt.ac.cn.

Author Contributions

‡These authors contributed equally to this work.

Notes

The authors declare no competing financial interest.

ACKNOWLEDGMENTS

This work was supported by National Program on Key Basic Research Project of China (973 Program) (MOST2011CB935700), the "100 talents" program of Chinese Academy of Sciences, the National Natural Science Foundation (Grant 20802039, 20901044, and 20902052), the Shandong Province Natural Science Foundation (Grant ZR2011BQ024 ZR2009BM014, BS2009NJ013, ZR2010BM016).

REFERENCES

(1) O'Regan, B.; Grätzel, M. *Nature* **1991**, *353*, 737.
(2) Grätzel, M. *Nature* **2001**, *414*, 338.
(3) Peter, L. M. *Phys. Chem. Chem. Phys.* **2007**, *9*, 2630.
(4) Yang, N.; Zhai, J.; Wang, D.; Chen, Y.; Jiang, L. *ACS Nano* **2010**, *4*, 887.
(5) Wang, X.; Zhi, L.; Müellen, K. *Nano Lett.* **2008**, *8*, 323.
(6) Halme, J.; Toivola, M.; Tolvanen, A.; Lund, P. *Sol. Energy Mater. Sol. Cells* **2006**, *90*, 872.
(7) (a) Papageorgiou, N. *Coord. Chem. Rev.* **2004**, *248*, 1421. (b) Olsen, E.; Hagen, G.; Lindquist, S. E. *Sol. Energy Mater. Sol. Cells* **2000**, *63*, 267.
(8) Wu, M.; Lin, X.; Wang, T.; Qiu, J.; Ma, T. *Energy Environ. Sci.* **2011**, *4*, 2308.
(9) Ramasamy, E.; Chun, J.; Lee, J. *Carbon* **2010**, *48*, 4556.
(10) Roy-Mayhew, J. D.; Bozym, D. J.; Punckt, C.; Aksay, I. A. *ACS Nano* **2010**, *4*, 6203.
(11) (a) Zhu, H. W.; Zeng, H.; Subramanian, V.; Masarapu, C.; Hung, K. H.; Wei, B. *Nanotechnology* **2008**, *19*, 465204. (b) Suzuki, K.; Yamaguchi, M.; Kumagai, M.; Yanagida, S. *Chem. Lett.* **2003**, *32*, 28. (c) Lee, W. J.; Ramasamy, E.; Lee, D. Y.; Song, J. S. *ACS Appl. Mater. Interfaces* **2009**, *1*, 1145.
(12) Ramasamy, E.; Lee, W. J.; Lee, D. Y.; Song, J. S. *Electrochem. Commun.* **2008**, *10*, 1087.
(13) (a) Li, Z.; Ye, B.; Hu, X.; Ma, X.; Zhang, X.; Deng, Y. *Electrochem. Commun.* **2009**, *11*, 1768. (b) Ameen, S.; Akhtar, M. S.; Kim, Y. S.; Yang, O. B.; Shin, H. S. *J. Phys. Chem. C* **2010**, *114*, 4760. (c) Jeon, S. S.; Kim, C.; Ko, J.; Im, S. S. *J. Mater. Chem.* **2011**, *21*, 8146.
(14) (a) Lee, K. S.; Lee, H. K.; Wang, D. H.; Park, N. G.; Lee, J. Y.; Park, O. O.; Park, J. H. *Chem. Commun.* **2010**, *46*, 4505. (b) Pringle, J. M.; Armel, V.; MacFarlane, D. R. *Chem. Commun.* **2010**, *46*, 5367. (c) Chen, J. G.; Wei, H. Y.; Ho, K. C. *Sol. Energy Mater. Sol. Cells* **2007**, *91*, 1472. (d) Xia, J.; Masaki, N.; Jiang, K.; Yanagida, S. *J. Mater. Chem.* **2007**, *17*, 2845.
(15) Wu, M.; Zhang, Q.; Xiao, J.; Ma, C; Lin, X.; Miao, C.; He, Y.; Gao, Y.; Hagfeldt, A.; Ma, T. *J. Mater. Chem.* **2011**, *21*, 10761.
(16) Li, G. R.; Song, J.; Pan, G. L.; Gao, X. P. *Energy Environ. Sci.* **2011**, *4*, 1680.
(17) Jiang, Q. W.; Li, G. R.; Gao, X. P. *Chem. Commun.* **2009**, 6720.

(18) Jang, J. S.; Ham, D. J.; Ramasamy, E.; Lee, J.; Lee, J. S. *Chem. Commun.* **2010**, *46*, 8600.
(19) Wu, M.; Lin, X.; Hagfeldt, A.; Ma, T. *Angew. Chem., Int. Ed.* **2011**, *50*, 3520.
(20) Wang, M.; Anghel, A. M.; Marsan, B.; Ha, N. L.C.; Pootrakulchote, N.; Zakeeruddin, S. M.; Grätzel, M. *J. Am. Chem. Soc.* **2009**, *131*, 15976.
(21) Sakurai, S.; Jiang, H.; Takahashi, M.; Kobayashi, K. *Electrochim. Acta* **2009**, *54*, 5463.
(22) (a) Wen, Z.; Cui, S.; Pu, H.; Mao, S.; Yu, K.; Feng, X.; Chen, J. *Adv. Mater.* **2011**, *23*, 5445. (b) Feng, Y.; He, T.; Alonso-Vante, N. *Chem. Mater.* **2008**, *20*, 26.
(23) Wang, Y. *J. Phys.: Conf. Ser.* **2009**, *152*, 012023.
(24) (a) Muto, T.; Ikegami, M.; Miyasaka, T. *J. Electrochem. Soc.* **2010**, *157*, B1195. (b) Fan, B.; Mei, X.; Sun, K.; Ouyang, J. *Appl. Phys. Lett.* **2008**, *93*, 143103. (c) Sudhagar, P.; Nagarajan, S.; Lee, Y. G.; Song, D.; Son, T.; Cho, W.; Heo, M.; Lee, K.; Won, J.; Kang, Y. S. *ACS Appl. Mater. Interfaces* **2011**, *3*, 1838. (d) Hong, W.; Xu, Y.; Lu, G.; Li, C.; Shi, G. *Electrochem. Commun.* **2008**, *10*, 1555.
(25) Dong, S.; Chen, X.; Gu, L.; Zhou, X.; Xu, H.; Wang, H.; Liu, Z.; Han, P.; Yao, J.; Wang, L.; Cui, G. *ACS Appl. Mater. Interfaces* **2011**, *3*, 93.
(26) (a) Kim, S. S.; Nah, Y. C.; Noh, Y. Y.; Jo, J.; Kim, D. Y. *Electrochim. Acta* **2006**, *51*, 3814. (b) Sakurai, S.; Jiang, H.; Takahashi, M.; Kobayashi, K. *Electrochim. Acta* **2009**, *54*, 5463.
(27) Popov, A. I.; Geske, D. H. *J. Am. Chem. Soc.* **1958**, *80*, 1340.
(28) (a) Yen, M.-Y.; Teng, C.-C.; Hsiao, M.-C.; Liu, P.-I; Chuang, W.-P.; Ma, C.-C. M.; Hsieh, C.-K.; Tsai, M.-C.; Tsai, C.-H. *J. Mater. Chem.* **2011**, *21*, 12880. (b) Yeha, M.-H.; Leea, C.-P.; Lina, L.-Y.; Niena, P.-C.; Chena, P.-Y.; Vittal, R.; Hoa, K.-C. *Electrochim. Acta* **2011**, *56*, 6157. (c) Zhang, J.; Li, X.; Guo, W.; Hreid, T.; Hou, J.; Su, H.; Yuan, Z. *Electrochim. Acta* **2011**, *56*, 3147. (d) Ramasamy, E.; Lee, J. *Carbon* **2010**, *48*, 3715.
(29) Saito, Y.; Kitamura, T.; Wada, Y.; Yanagida, S. *Chem. Lett.* **2002**, *31*, 1060.
(30) Sun, H.; Qin, D.; Huang, S.; Guo, X.; Li, D.; Luo, Y.; Meng, Q. *Energy Environ. Sci.* **2011**, *4*, 2630.
(31) Fabregat-Santiago, F.; Bisquert, J.; Palomares, E.; Otero, L.; Kuang, D.; Zakeeruddin, S. M.; Grätzel, M. *J. Phys. Chem. C* **2007**, *111*, 6550.
(32) Dao, V.; Kim, S.; Choi, H.; Kin, J; Park, H.; Lee, J. *J. Phys. Chem. C* **2011**, *115*, 25529.